Published by Avanti Publishers

International Journal of Petroleum Technology

ISSN (online): 2409-787X

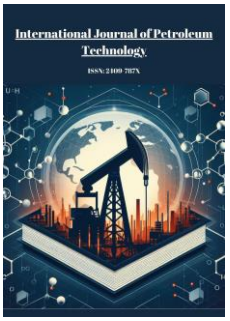

Stability and Process Optimization of Heavy Crude Oil Desalting Systems: Operational and Simulation-based Analysis

Miguel López-Patiño[1], Marinee Figueroa[1], Victoria Salazar-Palencia[1], Shirley Marfisi-Valladares[1,*], José Rengel-Hernández[1], Mario Lobo[2], Alix Guerrero[2] and Carlos Carvajal[2]

[1]*Universidad de Oriente, Departamento de Ingeniería Química, Laboratorio de Sistemas Dispersos y Ambiente, Grupo Sistemas Dispersos y Electroquímica, Barcelona, Venezuela.*

[2]*Servicios Enviroil C.A., Laboratorio Formulaciones Tensioactivas, Unidad de Investigación y Desarrollo, Barcelona, Venezuela.*

ARTICLE INFO

Article Type: Research Article

Academic Editor: Hao Zhang

Keywords:
Demulsifier optimization
Heavy crude oil desalting
Emulsion stability analysis
Electrostatic desalting process
Process simulation and optimization

Timeline:
Received: April 29, 2026
Accepted: June 01, 2026
Published: June 16, 2026

Citation: López-Patiño M, Figueroa M, Salazar-Palencia V, Marfisi-Valladares S, Rengel-Hernández J, Lobo M, Guerrero A, Carvajal C. Stability and Process Optimization of Heavy Crude Oil Desalting Systems: Operational and Simulation-based Analysis. Int J Pet Technol. 2026; 13(1): 29-44.

DOI: https: //doi.org/10.15377/2409-787X.2026.13.3

ABSTRACT

Process integrity is paramount in the oil industry to ensure operational reliability, safety, efficiency, and profitability. This is particularly vital in the Orinoco Oil Belt, the world's largest heavy and extra-heavy crude reserve, where the inherent properties of the resource impose strict requirements on its transportation, processing, and marketing. Consequently, this study performs an emulsion stability analysis to optimize the desalting process for these specific crudes. The methodology combines lab experiments, plant data analysis, and computer simulation of the process. The study results provide new insights to achieve this goal, such as: 1) Advanced modeling: Combining computer simulations and statistical analysis to map fluid thermodynamic and hydraulic behaviors. 2) Flow-mechanical insights: Correlating mixing valve pressure drops directly with emulsion stability. 3) Targeted parameter adjustments: Setting specific limits for heavy crude processing, including wash water pH, demulsifier concentration, and pressure thresholds to prevent gasification in electrostatic desalters. 4) Dynamic flow control: Upgrading mixing dynamics via optimized valves, control loops, and a new chemical injection system. 5) System stabilization: Resolving industry constraints through targeted mechanical and automation enhancements that ensure process integrity and predictable operations.

*Corresponding Author

Emails: marfisi.shirley@gmail.com; smafisi@udo.edu.ve

1. Introduction

In the petroleum industry, crude oils of different qualities are processed and refined to obtain high-value derivative products (gasoline, diesel, naphtha, and lubricants, among others). To remove impurities such as water, sediments, and inorganic salts, conditioning processes known as dehydration and desalting are employed. Extra-heavy crudes (< 10 °API), require prior dilution with solvents (naphtha or lighter crudes) and other technologies (hydrotreating and thermal conversion) to increase their refining capacity and commercial quality. Thus, crude upgraders are developed to meet the following objectives: a) To produce a diluted crude oil (DCO) that can be transported through pipelines; b) To optimize its properties (viscosity, water and sediment content, sulfur, nitrogen, metals, and Conradson carbon); and c) To market a higher-value improved crude (22-32 °API).

In Venezuela, crude upgraders produce synthetic crudes through the integration of several process plants. The crude unit, where desalting and fractionation processes (atmospheric distillation and vacuum distillation) are carried out; the delayed coking unit, where coke is obtained as a by-product; the hydrotreating and hydrocracking units, which use hydrogen and catalysts to upgrade gas oils and remove impurities; and the industrial utilities units and environmental plants for waste management. In these units, fluid heating is provided by preheating trains, comprising heat exchangers that recover heat from product streams and recirculation, transferring it to the feed streams to achieve the required operating temperature in the equipment.

The desalting process in upgraders is carried out in electrostatic treaters, custom-built to meet specifications for water and salt content. The feed is composed of two streams (crude oil and wash water) that are pre-mixed to form a low-stability water-in-oil (W/O) emulsion. The application of an electric field accelerates the first stage of emulsion breaking, characterized by the initial approach of the water droplets and the formation of induced dipoles (stage 1). Followed by the destabilization of the interfacial film and the drainage of the inter-droplet oil by the action of the demulsifier (stage 2) until coalescence and separation by gravitational sedimentation (stage 3), as explained by Cottrell and Speed in 1911 [1]. In this equipment, the removal of water and salts occurs in a short time with high efficiency [2-7].

The demulsifier modifies the interfacial properties (tension, modulus of elasticity, and viscosity) to allow coalescence to proceed [8-11]. It is a commercial product, formulated with a mixture of polymeric surfactants in an organic medium (an aliphatic-aromatic hydrocarbon solvent) that allows for its molecular diffusion through the crude oil (continuous phase) and adsorption at the interface of the water droplets (dispersed phase) of the emulsion. The types of surfactants and formulation protocols have been referenced in various investigations [12-16], in addition to optimal correlation parameters as criteria for emulsion breaking [17].

Recent studies [18-22] have reviewed the emulsion destabilization process and its associated problems, providing a theoretical basis and technical support for the application of cutting-edge technologies. The salt content in the crude oil is an important parameter for controlling corrosion at the overhead and internals of atmospheric and vacuum distillation columns, manifested as consequence of the hydrogen chloride vapor formed in salt hydrolysis reactions at high temperatures. Furthermore, sodium ions cause catalyst poisoning in hydrotreating units [23, 24].

From this perspective, proper crude desalting is fundamental before its upgrading or refining. For this reason, the objective of this work was to perform a stability analysis of the desalting process of a heavy crude oil, which presented values outside of specification regarding the salt content of the desalted crude. To this end, laboratory and field studies were conducted to identify the causes and establish solutions, considering the following optimization approaches:

- One-dimensional analysis for the identification of key variables and statistical control.
- Efficiency tests to determine the optimal demulsifier concentration in the presence of variations in wash water quality.
- Sensitivity analysis based on flow diagrams, material balances, and simulations of fluid behavior under changes in operating variables, establishing process limitations and improvements.

2. Materials And Methods

An applied research design was employed combining field surveys and laboratory tests to determine the critical variables in the desalting system of a crude upgrader located at the "José Antonio Anzoátegui" Cryogenic and Petrochemical Complex in Anzoátegui State, Venezuela. The separation process at these facilities is carried out using dual-polarity electrostatic desalters (EDGE model manufactured by FORUM Energy Technologies; dimensions: 1,762.3 ft^3 capacity, 104 ft T/T length, and 12 ft internal diameter). This equipment utilizes a high-voltage electric field and AC/DC current between pairs of metallic electrodes (vertical plates) to produce electro-coalescence of water droplets in a short time.

Fresh samples of crude oil and wash water were collected on-site and characterized using the procedures described in ASTM [25-27] and APHA [28-32] methods (American Public Health Association, 2023). The analysis methods and the measured values of the characteristic properties are indicated in the Appendix, Table **A1**. The wash water originated from three sources: the bottom of the sour water stripper, the atmospheric tower overhead accumulator, and the vacuum tower overhead drum. The heavy crude oil (17 °API), consisting of a blend of extra-heavy crude (8 °API) diluted with naphtha, comes from the oil fields of the Orinoco Oil Belt (FPO) and is dehydrated at the main fluid processing station, from where it is sent to the crude upgrader. The methodology used in the study is described in the following sections.

2.1. One-dimensional Statistical Analysis

One-dimensional statistical analysis examines a single variable at a time in a dataset. It involves collecting, organizing, analyzing, and presenting data, and follows the rules of probability. It interprets key statistical measures like central tendency (mean, median, mode), dispersion (range, variance, standard deviation), skewness, and kurtosis.

For the study, a representative population of 1,040 data points per variable was considered, collected from the company's database LIMS (Centralized Information Synchronization and Emission) and Aspen Process Explorer™ over a period of 36 months, with daily sampling frequency and variable data ranges depending on each parameter. As an initial criterion for data cleaning, values were discarded when the crude oil volumetric flow was below 140 MBPSD, as this represents an unstable operating condition.

Data processing was performed using Statgraphics® software. It was based on validating the assumption of normality and the alternative modeling of non-parametric variables through specific distributions (inverse Gaussian, minimum extreme value, or log-logistic). The analysis consisted of five sequential stages: a) cleaning of outlier data; b) applying normality tests; c) parametric optimization; d) alternative models and signal smoothing; e) calculation of central tendency metrics and control limits for process monitoring.

2.2. Efficiency Tests

Formulation sweeps were conducted by changing one variable at a time while keeping the others constant [35], in order to understand the effect caused by varying the wash water pH (formulation variable) and the demulsifier concentration (composition variable) on the destabilization of the emulsion [36]. The experimental design was based on a multifactorial analysis [33, 34], with the factors being pH with 7 levels between 5 and 11 (values recorded in the plant for effluent waters used as wash water and measured with a Metrohm 691 digital meter), and the demulsifier concentration with 7 levels between 3 to 21 ppm (recommended range by the supplier, including the value used in the plant of 9 ppm), for a total of 7^2 SOW (surfactant/oil/water) systems. The response variable was stability (tc), measured as the time required to separate 50% of the coalesced aqueous phase volume (Vc) relative to the initial aqueous phase ($V\infty$) in the emulsion; comparing it against the blank (emulsion without demulsifier).

In the preparation of each system, 100-mL capacity Pyrex centrifuge tubes were labeled and placed in racks, adding 100 mL of W/O emulsion formed with 94.5% crude oil and 5.5% water (previously preheated and characterized) under gentle agitation (KAM Controls non-aerating mixer). The water pH range was obtained by

adding acid or base to the water. The commercial demulsifier, diluted to 10% w/v in xylene, was added using a micropipette (previously calibrated, where 1.0 mL is equivalent to 1.0 ppm). Then, the tubes were capped and manually shaken until homogenized, heated, and left to settle at 180 °F in a thermal bath (Precision, manufactured by Scientific Petroleum Instruments); see Appendix, Fig. **A1**. The volume of separated water at the bottom of each tube was recorded at each time interval from 0 to 300 min. From these data, coalescence plots (Vc/V∞ *versus* time) and stability plots (tc *versus* concentration and pH) were constructed to determine the optimal pH and demulsifier concentration values under laboratory conditions.

Efficiency tests were also conducted by varying the demulsifier concentration (known as the bottle test) using a laboratory electrostatic desalter (Electrostatic Dehydration Tester InterAV. Inc.), applying a voltage of 3 kV in 5-minute intervals for 30 min and recording the separated water volume over 60 min (see Appendix, Fig. **A2**), to more closely simulate the conditions within the electrostatic desalters. The mixing of the crude oil and the wash water (pH adjusted to 7) was performed using an Ultraturrax homogenizer at 6,000 rpm for 3 s, after preheating at 180 ºF for 20 min in a thermostatic bath, followed by 30 min on a shaker (mechanical agitator) for the homogenization of the fresh samples [36]. The measurement of the residual water content was carried out according to the ASTM D 4007-22 procedure [27].

2.3. Sensitivity Analysis

A computational tool was developed to perform variations in the operational variables that affect the desalting process, such as agitation and mixing (mixing efficiency), wash water and feed crude flow rates, salinity, and water content in the crude, as shown in Fig. **1**. The tool determines the salt content in the crude at the outlet of the second desalting unit, using an iterative trial-and-error cycle, with a relative error of 0.0%. The procedure consisted of the following steps:

a) Establish the material balance equations, global (eq. 1) and by components (eq. 2) for the process accounting in two stages, considering two desalting units (Fig. **1**).

b) With an iterative loop, the unknown currents are determined, using as a stopping criterion the variable whose estimated value equals the experimental value. In this case, it's the salt content of the desalted crude in the first stage. Perform the sensitivity analysis by perturbing one variable at a time per analysis, within a predetermined range.

c) Calculate the process efficiency (Eqs. 3 and 4).

d) Generate the results report.

$$\sum_{i=1}^{n} \dot{F}_{entrada} = \sum_{i=1}^{n} \dot{F}_{salida} \tag{1}$$

$$\sum_{i=1}^{n} (x_i \dot{F})_{entrada} = \sum_{i=1}^{n} (x_i \dot{F})_{salida} \tag{2}$$

$$\%E1 = \left(\frac{PTB_{entrada} - PTB_{salida}}{PTB_{entrada}}\right) x100 \tag{3}$$

$$\%E2 = \left(\frac{BSW_{entrada} - BSW_{salida}}{BSW_{entrada}}\right) x100 \tag{4}$$

Where $\dot{F}$: mass flow of the inlet and outlet streams to each dehydration unit, considering a balance without chemical reaction, x_i: mass fraction of each component, PTB is the salt concentration in PTB (= lb salt/1,000 BPD crude), BSW: water and sediment content in %v/v, E1: Desalting efficiency; E2: Dehydration efficiency.

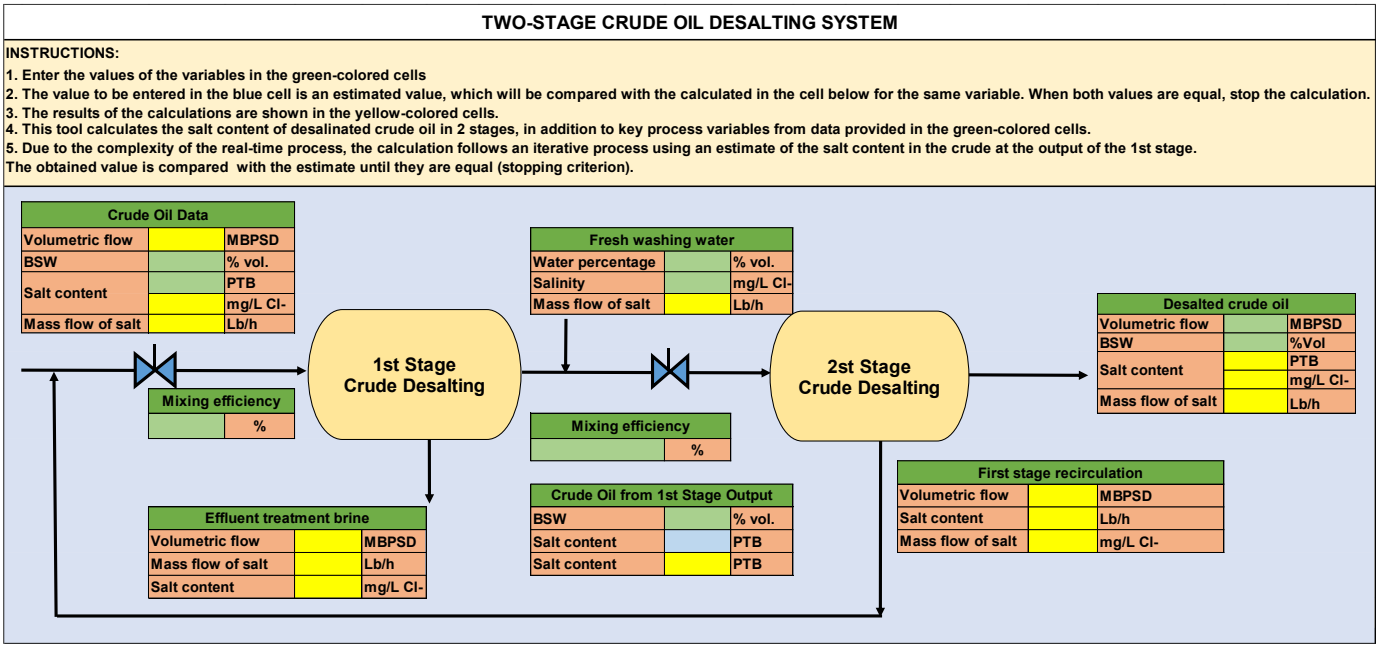

Figure 1: Schematic of the calculation tool for two-stage crude oil desalting.

Fig. (**1**) shows a diagram of the two-stage desalting process, identifying the variables in the inlet and outlet streams, as well as the user instructions for data entry into the calculation tool. The process occurs as follows: The feed crude is mixed with the water separated from the second stage, forming a W/O emulsion at the first mixing valve, which is then treated in the first-stage desalters, and the separated water is drained to the treatment system. The partially dehydrated and desalted crude is mixed again with wash water (low-salinity fresh water) at the second mixing valve, and the emulsion enters the second desalting stage for final removal to reach quality specifications, according to the design criteria of < 2 PTB (pounds of salt per thousand barrels of crude) and < 1.0% BSW (basic sediment and water). The demulsifier is injected at the inlet of the preheating train to ensure a longer contact time.

To validate the calculation tool, the estimated salinity of the desalted crude oil was compared with the measured value (Herzog SC-960 analyzer), reported in Table **A2** of the Appendix. The procedure was as follows:

a) Measurement of the salt content in the inlet and outlet streams of the desalting trains for the collected samples (wash water, effluent water, crude oil).

b) Selection of the diluted crude volumetric flow per train and the water/oil ratio, using real-time monitoring data and the Aspen Process Explorer® simulator.

c) Mass balance considering two cases: 1) Iterations until the salt concentration in the desalted crude oil corresponds to the measured value. 2) Applying another iterative process that assumes the measured salt value in the effluent water (water separated in the first desalting stage), calculating the salt content in the desalted crude.

2.4. Technical Evaluation of Proposals

The following are the proposals to improve the crude oil desalting process, along with the methodology used to evaluate their technical feasibility based on operational performance, adjustments, and changes in the control philosophy.

Pressure control in the crude oil stream at the inlet of the desalting system: First, the formation of vapor phase in the liquid zone was verified, estimating the bubble point pressure of the feed stream under the design and normal operation cases (values reported in the Appendix, Table **A-2**). The bubble point curve was generated

(Appendix, Fig. **A3**), using the AVEVA PRO/II® process simulator and the Peng-Robinson equation of state, with the operating limits set as follows:

a) Pressure in the second desalting stage must be 20 psi max above the bubble point pressure (equipment manufacturer's recommendation) to prevent the evaporation of light fractions and increased water carryover at the top of the atmospheric column.

b) Operating pressure in the first desalting stage must consider the maximum pressure drop contributed by the mixing valves (20 psi) and the desalters (3 psi per vessel, at maximum load), neglecting pressure losses through piping (section with length inferior to 6 m). Valve manufacturers were consulted on the feasibility of changing the current technology of the ball-type valve (1.64 ft diameter, Cv 1,003, normal operating) for a globe-type valve, establishing the operating conditions as a function of the design values for the cases of minimum, normal, and maximum operating flow rate in the plant. The available connections to incorporate pressure transmitters were identified.

Crude oil flow control at the outlet of the desalting system: Through an on-site inspection, the state of the flow control valves in the first and the second desalting trains, and the feed valve to the preflash tower, was evaluated. For the adaptation of the control loop, tests were performed in the plant's control system, adjusting loop-response time to avoid disturbances that could generate increases in the operating pressure of the atmospheric distillation column.

Flow control of the wash water from the vacuum overhead accumulator: For this purpose, the sizing of a flow control valve was performed using the following criteria:

- Valve flow coefficient (CV_L) calculated by Eq. 5
- Control valves with an opening percentage between 15% and 80%
- Control valve outlet velocity ≤ 30 ft/s
- Pressure differential across the control valve < 15 psi
- Control valves without flashing or cavitation
- Control valve noise lower than 85 dB
- Control valve bypass valves of the globe type if $\Delta P > 10.2$ psi; otherwise, butterfly type.

$$CV_L = \frac{W_L}{63.5 \times \sqrt{\rho \times \Delta P}} \tag{5}$$

Where: ρ is the density of the fluid at upstream conditions of the valve (lb/ft³), W_L is the liquid mass flow (lb/h), and ΔP is the pressure drop across the valve (psi).

Hydraulic simulations for the estimation of pressure drops in the piping were performed with the Pipephase® program, defined as Network–Liquid with the Beggs-Brill-Moody flow correlation. The required pressure at the mixing point of water and crude oil was established at 212 psig under normal condition and 225 psig under maximum condition (when sludge washing is performed).

Demulsifier injection package: This proposal contemplated the design of a demulsifier injection system, performing a review of supplier proposals to select demulsifiers, dosage ranges, and location. From this information, the preliminary process and piping and instrumentation diagrams were generated.

Sludge washing of the desalters: It consisted of the verification of the operational procedure [37] performed in the desalters, highlighting the following aspects:

- Sludge washing per tap: 7 min (three taps per equipment), starting in the first desalter of the train being washed and continuing with the second desalter.

- Operating conditions: temperature in the desalter between 275 °F and 340 °F, wash water flow rate per tap of 217 gpm, outlet pressure in the valves of 224 psig, and interface level in the second level tap (level control is manual).
- Oil and grease analysis, before and after the sludge washing, applying the procedure described in the standard SM 5520-C [32].

3. Results

In Tables **1a**, **1b**, **1c**, and **2**, the one-dimensional analysis of the key variables involved in the heavy crude oil desalting process is presented, identifying the measures of central tendency (mean, median, and mode), control limits, range (minimum and maximum), and design. The mean represents the average of the data, the median is the central value, and the mode is the value that repeats most frequently in the data set.

Table 1a: Statistical analysis of the key variables in the crude oil desalting system.

Statistical analysis	Crude oil feed stream to electrostatic desalters				Sour wash water	
	Total feed flow (MBPSD)	Flow rate per train (MBPSD)	Temperature (°F)	Pressure (psig)	Temperature (°F)	Pressure (psig)
Mean	183.0	85.9 / 95.8	266.0	171.0	219.3	220.1
Median	180.0	85.9 / 94.2	262.6	170.6	219.2	219.7
Mode	200.0	--	262.3	--	--	--
UCL: +3σ	--	122.2 / 104.9	329.3	185.5	263.0	251.6
LCL: -3σ	--	33.5 / 86.8	243.1	152.8	175.7	208.7
Minimum	140.0	50.3 / 50.4	238.5	141.8	179.5	113.0
Maximum	235.0	114.4 / 124.5	309.3	189.0	264.2	297.6
Design	247.6	130.0 / 130.0	307.0	190.0	240.0	280.0
Power	Not applicable	Not applicable	Not appl.	3,337	Not applicable	Not appl.
Distribution	Normal	Weibull / Normal	Largest extreme value	Normal	Logistics	Largest extreme value

Table 1b: Statistical analysis of the key variables in the crude oil desalting system.

Statistical analysis	Interface level (%) in desalters				ΔP in mixing valves (psi)			
	D1A	D1B	D2A	D2B	D1A	D1B	D2A	D2B
Mean	50.0	50.0	50.0	50.0	12.9	12.7	13.1	12.9
Median	50.0	50.0	50.0	50.0	12.9	12.4	12.9	13.0
Mode	53.1	52.0	52.1	52.0	17.4	17.5	17.1	17.3
UCL: +3σ	46.9	48.0	47.9	48.0	5.6	5.2	6.2	5.9
LCL: -3σ	45.4	36.5	39.1	35.0	6.0	5.6	7.3	7.4
Minimum	56.9	66.9	55.5	55.1	18.0	17.4	17.3	16.8
Maximum	65.0	65.0	65.0	65.0	5-20	5-20	5-20	5-20
Power	Not applicable	Not applicable	Not applicable	Not applicable	Not applicable	1.57	2.50	1.97
Distribution	Laplace	Laplace	Laplace	Laplace	Weibull	Weibull	Weibull	Weibull

D1A and D1B: electrostatic desalters of the first desalting train; D2A and D2B: electrostatic desalters of the second desalting train; ΔP: pressure differential across the mixing valves.

Table 1c: Statistical analysis of the key variables in the crude oil desalting system.

Statistical analysis	Voltage/Current 16 kV(V / Ω)				WOR (%)		Efficiency on Trains 1 and 2		
	D1A	D1B	D2A	D2B	D1B	D2B	E1 (%)	E2 (%)	Oil in water (mg/L)
Mean	3751.6 15.7	3879.6 15.9	3737.1 14.5	3356.2 14.7	5.5	5.5	77.5 77.8	87.1 88.6	580.2 569.9
Median	3758.0 17.9	3878.5 16.0	3758.0 16.3	3351.3 14.8	5.5	5.5	77.8 77.7	87.7 89.4	563.5 555.0
Mode	3780.2 15.9	-	37,81.2 15.5	3403.1 13.8	--	--	76.0 77.0	88.3 90.7	481.2 477.7
UCL: +3σ	3921.6 24.9	3925.3 27.4	3914.4 33.1	3644.2 30.0	7.6	7.6			
LCL: -3σ	3285.5 9.9	3834.7 9.1	3412.0 10.5	2559.1 9.2	3.4	3.4			
Minimum	2993.5 11.48	2737.5 9.65	2785.5 5.29	2823.8 9.5	3.9	3.5			
Maximum	3914.4 30.7	3929.0 24.6	3546.0 35.5	3619,5 23,6	8.3	8.2			
Mean	> 4000 < 20.0	> 4000 < 20.0	> 4000 < 20.0	> 4000 < 20.0	6.0 7.0	6.0 7.0	98.0	93.8	600.0
Power	Not appl.	Not appl.	Not appl.	Not appl.	Not appl.	Not appl.	Not appl.	Not appl.	Not applicable
Distribution	Weibull	Gaussian a inversa or Log-logística	Smallest or largest extreme value	Smallest or largest extreme value	Laplace	Laplace	Weibull or Normal	Smallest extreme value	Largest extreme value

D1A and D1B: electrostatic desalters of the first desalting train; D2A and D2B: electrostatic desalters of the second desalting train; WOR: water to oil volumetric ratio; E1: Desalting efficiency; E2: Dehydration efficiency.

Table 2: Statistical analysis of the laboratory variables in the desalting system.

Statistical analysis	Crude oil feed stream to electrostatic desalters				Desalted crude oil per train	
	Salt content (PTB)	BSW (% v/v)	Gravity (°API)	Total acidity (mg KOH/g)	Salt content (PTB)	BSW (% v/v)
Mean	51.9	1.3	16.4	3.0	11.2 / 11.2	0.9 / 0.8
Median	50.0	1.2	16.3	3.0	11.4 / 11.3	0.8 / 0.8
Mode	50.0	1.0	16.0	3.0	11.2 / 11.2	0.8 / 0.7
UCL: +3σ	27.0	0.4	15.3	2.3	2.9 / 3.1	0.5 / 0.3
LCL: -3σ	200.0	3.2	17.4	3.8	25.1 / 27.9	1.5 / 1.8
Minimum	100.0	1.0	16.0	2.7	< 2.0	< 1.0
Power	Not appl.	Not appl.	Not appl.	Not appl.	Not appl.	Not appl.
Distribution	Inverse Gaussian	Log-logistics	Inverse Gaussian	Laplace	Log-logistics Log-logistics	Inverse Gaussian Largest extreme value

Fig. (**2**) shows the stability plot as a function of the demulsifier concentration by varying the pH of the wash water in the formulation-composition scan, under the conditions simulated in the laboratory. The dashed lines highlight the optimal demulsifier concentration value to separate half of the aqueous phase, which increases at basic pH.

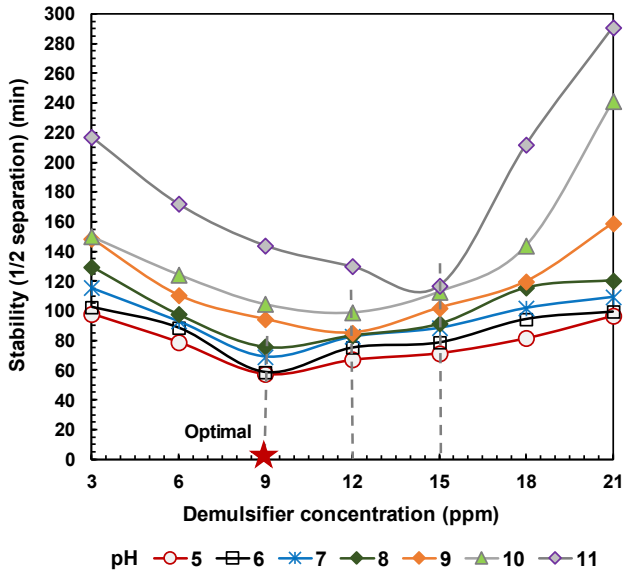

Figure 2: Emulsion stability as a function of the demulsifier concentration, varying the pH of the wash water (one-dimensional scans at 180 °F, 14.7 psi).

Fig. (**3**) shows images of the W/O emulsion before and after adjusting the pH of the sour water in the efficiency test with a laboratory electrostatic dehydrator, combining various treatment methods (heat, electric field, and demulsifier) under simulated field conditions.

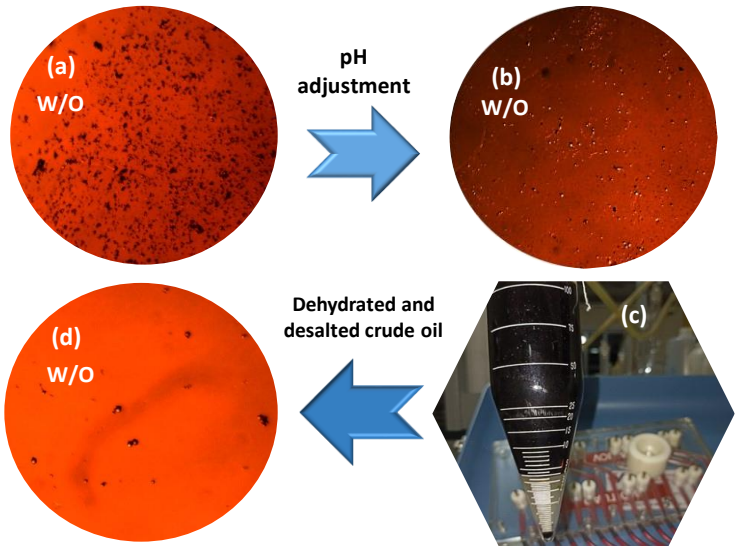

a) Emulsion formed with fresh samples of heavy crude oil and sour wash water (pH 9.1). **b)** Emulsion formed after adjusting the pH in the wash water. **c)** Electrolytic cell with separated phases, smooth interface, clear water, without residual emulsion and sediments at the bottom. **d)** Dehydrated crude oil showing a reduced number of water droplets with asphaltenic residues. The images were captured with an optical microscope (Motic SMZ-168, with transmitted superimposed light, 0.65X lens, and 5X zoom adjustment).

Figure 3: Micrographs of the W/O emulsion in the efficiency test, employing a laboratory electrostatic dehydrator under simulated field conditions (3 kV for 30 min, 180 °F, 14.7 psi).

Table **3** records the measured salt content values of the inlet and outlet streams in the desalters under current operating conditions, reporting the efficiency achieved in the crude oil desalting, before optimization. Table **4** shows the optimized values after implementing the improvements to increase efficiency in the desalting process.

Table 3: Salt content measured and efficiency under operating conditions.

Inlet/outlet flow in desalters	Salinity	Efficiency E1 (%)
Wash water to electrostatic desalters	24.0 mg/L	-
Crude oil to electrostatic desalters	58.1 PTB	
Salt water separated on Train 1	1758.0 mg/L	-
Salt water separated on Train 2	1866.0 mg/L	-
Crude oil desalted in the D1A desalter	15.7 PTB	74.2
Crude oil desalted in the D2A desalter	15.0 PTB	73.0
Crude oil desalted in the D1B desalter	10.5 PTB	83.7
Crude oil desalted in the D2B desalter	9.5 PTB	81.9

Deviation: salinity ± 0.1 (ASTM D3230). E1: Desalting efficiency.

Table 4: Optimized values after improvements in the desalting system.

Parameter	Value
Initial desalting efficiency, %	74.0
Final optimized efficiency, %	86.0
Reduction in salt content, PTB	50.0
Improvement percentages, %	12.0

4. Discussion

4.1. Interpretation of the Key Variables in the Desalting Process

The impact of key parameters for the optimization of crude oil desalting has been analyzed by several researchers [38-41], showing specific responses in each system, due to the particularities of the crude segregations and the quality of washing water in desalting systems. This, together with failures in the heat transfer systems and the availability of automated control devices and instruments to mitigate these fluctuations, causes significant process variability. Therefore, periodic assessment of the behavior of key variables is crucial to minimize instability conditions in the system.

Crude oil desalting relies on emulsion dehydration for phase separation; thus, it is feasible to categorize the key variables in terms of emulsion theory [35, 42]. That is, into formulation variables (temperature, nature of the crude oil, pH of the wash water), composition variables (water/oil ratio and demulsifier concentration), and flow-mechanical variables (flow rate, pressure, agitation, and mixing); in addition to other external variables (voltage/amperage, interface level).

The one-dimensional analysis of the operational data history, reported in Tables **1a**, **1b**, and **1c**, provides information on the measures of central tendency for statistical process control. The arithmetic mean and the lower (LCL) and upper (UCL) control limits defined the range of values for the variables, detecting out-of-control values with standard deviations of ± 3σ. An industrial process, under statistical control is considered mechanically stable if its variations are strictly confined within a range of three standard deviations from the mean [33]. The macroscopic interpretation of these results, from a mechanical and hydraulic perspective, is as follows:

- Loss of the safe operating range: The feed volumetric flow to the crude unit (manipulated variable according to plant requirements) had an average of 183 MBPSD, a mode of 200 MBPSD, and a maximum of 235 MBPSD, which is below the design (247.6 MBPSD); in addition, there were uneven flows (85.9 MBPSD and 95.8 MBPSD) in each train. The problem is that the flow variation causes instability in the interface level or height for effective water and crude separation. Regarding the average recorded temperature (262.6 °F), it was below the design (307 °F) due to the heat exchangers being out of service for maintenance. A lower

temperature increases the crude oil's viscosity and boosts the drag forces, which slows down the settling speed of coalesced water droplets according to Stokes' Law. As a result, it increases the residence time required for the complete resolution of the emulsion. Additionally, the thermal shock with the wash water in the mixing valve caused hydrodynamic instability in the system.

- Vaporization of light components due to low pressure: The drop in the average operating pressure to 171 psig (with minimums of 108–127 psig in the second stage), compared to the design value of 190 psig, along with the change in the diluent quality (naphtha from 47 °API to 60 °API), led to the vaporization of the lighter fractions. When the pressure dropped below the actual bubble point pressure (which exceeded the design value), it caused the instant gasification or vaporization of the light components inside the desalter. This vapor phase disrupted the flow pattern and induced short circuits due to electrical arcs (voltage drop < 4 kV and current peaks > 20 A) in the energized grids of the desalter [43-45].
- Instability in the mixing valve: Flow variations change the optimal differential pressure in the inlet mixing valve. If the flow drops, the pressure drop decreases and there isn’t enough hydraulic energy to mix the wash water with the crude. If the flow goes up too much, the hydraulic shear is so high that it creates an emulsion that takes more time or chemicals to break and coalesce electrostatically.
- Loss of desalting efficiency: For train 1, an arithmetic mean of 77.5% for desalting and 87.1% for dehydration was obtained. For train 2, an arithmetic mean of 77.7% for desalting and 88.6% for dehydration was achieved. Therefore, the desalted crude in both desalting trains is outside of the design specification (98% and 93.8%); the technology licensor recommends 95% and 98%, respectively. The increase in salinity to 27.9 PTB compared to the design value (< 2 PTB) is not a failure of the desaltin unit itself, but the direct result of the constraints of operating under conditions beyond the safe limits. The causes are diverse, ranging from equipment being out of operation due to mechanical failures, to fluctuations in the raw feed flow and free water stratification in the storage tanks. It's important to note that the tank mixers had a high history of failures.

4.2. Optimal Demulsifier Concentration

Fig. (**2**) shows a parabolic or 'V'-shaped curve with a stability minimum as the demulsifier concentration increases at a constant pH, which is characteristic of an emulsion destabilization process by surfactant action. A deficiency of demulsifier doesn't break the film, while an excess inverts the emulsion (O/W), acting as a secondary emulsifier. The minimum represents the critical point where the greatest water separation is achieved in the shortest possible time, corresponding to the optimal demulsifier concentration [35, 42]. For the studied system, pH variations in the wash water between 5 and 8 require 9 ppm of demulsifier to break the emulsion in a time of 57.5 to 75.8 min, respectively. At pH 9 and 10, it was 12 ppm with longer times (85.3 min and 99.0 min); while at pH 11, it demands 15 ppm and 117 min for phase separation.

Statistical analysis using the multiple range test method showed high variability in the response to changes in these two key variables. By varying the demulsifier concentration (3 to 21 ppm), the response variable (volume of separated water) presented three homogeneous groups of means with statistically significant differences, and the contrast of means between one level and another yielded five pairs of means with significant differences; in both cases at a 95% confidence level. When analyzing the pH variable (5 to 11), four homogeneous groups of means with statistically significant differences were identified; the contrast of means between one level and another reported eleven pairs that showed significant differences with a 95% confidence level. The response analysis reflected an optimal separation time of 66 min at pH 6 and 9 ppm of demulsifier.

The use of unconditioned sour water introduced critical contaminants that impacted the water-in-oil (W/O) emulsion stability and therefore, the electrostatic coalescence stage. Fig. (**3**) shows a significant amount of black flocs of varied sizes in the emulsion micrograph (Fig. **3a**). When taking an aliquot of this emulsion and bringing it into contact with xylene, the flocs dissolved, verifying that they corresponded to crude oil. Under this condition, it was not possible to resolve the emulsion by applying the electric field, making the conditioning of the wash water necessary (Fig. **3b**) to achieve the breaking process according to performance specifications [36]: completely separated phases, clear water, smooth and defined interface, without residual emulsion (Fig. **3c**), resulting in a dehydrated and partially desalted crude (Fig. **3d**).

Even after adjusting the pH to a neutral value, the desalting efficiency was 80% at a demulsifier concentration of 12 ppm and a settling time of 60 min. This result can be explained by the presence of other contaminants in the sour water that also affect the emulsion resolution and demand longer residence times. Table **A1** shows the characterization of the sour water, reflecting a chloride content of 54.6 mg/L, higher than the design value (< 25 mg/L), which interferes with the electro-coalescence process. An oil and grease contribution of 58.1 mg/L contributes to the segregation of lipophilic species in the interfacial zone and the hydrogen sulfide content of 64.6 mg/L, representing a risk due to its corrosive effects.

Ammoniacal nitrogen content of 477 mg/L can act as a cationic emulsifier, generating changes in the wettability of solids and/or the formation of anionic-cationic complexes, amines, and nitrosamines with negative effects on crude oil desalting and effluent water treatment. It is noteworthy that water with pH > 8 promotes the precipitation of corrosive and fouling solids that demand longer residence times [46], from about 66 min at pH 7 to 117 min at pH 11, being a critical factor due to damage to the desalter internals, effluent water discharge pumps, and downstream equipment, such as the atmospheric distillation column [24]. Sour water is potentially toxic and has a high impact on the environment, people, and the crude oil upgrading process activities themselves [47]. The design requirement calls for wash water that is free of oil and grease, hydrogen sulfide, and ammonia, with low salinity and a pH close to neutral.

4.3. System Behavior Under Operational Changes

Based on the sensitivity analysis, the effect of temperature fluctuations of the preheated feed crude (240 °F to 305 °F) on the increase of separated water occupying the crude oil zone was evaluated. At a 65% interface level, the minimum estimated temperature to avoid affecting this variable was 244 °F and 251 °F for a water/oil ratio of 6 and 7 %v/v, respectively, considering the fluid properties according to design. At a 50% interface level, between 244 °F and 265 °F is required, respectively, under normal operation. The rate of change must not exceed 5 °F in a 15-min period to avoid abrupt fluctuations.

The water/oil interface level (also expressed in % height) shows how much of the vessel space is occupied by water (below the interface level) and by oil (above the interface level). The level measurement instrument in the desalters is of the capacitive type, with a system of five trycocks per desalter for visual inspections to verify the height occupied by crude oil, water, or residual emulsion. High water levels lead to the percolation phenomenon and short circuits, interpreted by low or erratic voltage readings on the voltmeter. A low water level reduces the residence time in the equipment and leads to an increase in oil and grease in the effluent water sent to the water treatment unit.

The results in Table **3** reflect desalting efficiencies of 73% to 84%, which are unfavorable for downstream equipment, especially due to the impact on the metallurgy of the atmospheric distillation column overhead. Under these conditions, a dehydrated crude within specification (< 1.0 %v/v BSW) and partial desalting (9.5 to 15 PTB) are achieved, far from the quality criterion (< 2 PTB), which can be attributed to any of the following reasons:

- Insufficient mixing for the dilution and transport of brine droplets from the crude oil with the wash water. The mixing valve operates manually and depends on the operator to adjust the pressure differential according to the fluid flow rate entering the system. When low-salinity wash water is added, proper mixing must be ensured to: a) disperse the free water volume into droplets within the oil phase; b) integrate the brine droplets present in the feed crude; c) dissolve salt crystals; d) facilitate the adsorption of the demulsifier at the water/crude interface [48].
- High stability of the emulsion to be desalted due to restrictions in wash water quality (see Table **A1** and Fig. **3a**) or the entry of other streams (out-of-specification crude, slop oil) that demand a higher demulsifier dosage. In the efficiency tests with the laboratory electrostatic dehydrator, a requirement of 12 ppm was obtained with a longer settling time, after adjusting the sour water pH to a neutral value.
- High stability of the emulsion to be desalted due to restrictions in droplet size and shape (Fig. **3b**), and high salinity that opposes deformation (Laplace's Law). In general, the formation water associated with oil in the Orinoco Oil Belt reservoirs presents high salinity [36, 49, 50].

- Operating pressures between 108 psig and 127 psig (see Appendix, Table **A3**), indicating the vaporization of the lightest components. The minimum pressure to avoid vaporization in the second-stage desalters must be 135 psig. Given that there are no pressure transmitters available, the Fig. **A4** (see Appendix) is useful for operators to assign a set point value to the safety valve pressure controller, avoiding erratic behavior in level sensors.
- Calibration of the salt measurement equipment. Potentiometric quantification of salts in crude requires strict calibration of the equipment at different concentration ranges to avoid errors from signal saturation, as pointed out by ASTM D3230 [25]. Variations in the measured salt content compared to the value calculated in the mass balance showed deviations of up to 20%.

4.4. Improvements in the Desalting System with Process Optimization

Stabilization of the inlet pressure profile: Replacing the original ball-type valve (10-PV-153) with a globe valve reduced water hammer effects and increased modulation accuracy, keeping pressure fluctuations within a narrow range of 179.4 psig to 182.9 psig, successfully setting the set point at 181 psig. The incorporation of pressure transmitters in the desalters will ensure the system operates at the value recommended by the manufacturer (> 20 psig above the bubble point).

Reconfiguration of the crude feed control loop: Installation of two auto-manual station controllers that transmit the signal of opening percentage from the lower selector to the liquid level control valves (10-LIC-151) of the preflash chamber and to the pressure control valve (10-PIC-153B).

Increase in overall desalting and dehydration efficiency: By analytically optimizing the manual mixing valves, an optimal differential pressure drop of 10 to 12 psi was determined. This change boosted desalting efficiency to 86% and dehydration efficiency to 88% (see Table **4**), surpassing the previous historical averages of the process (see Table **3**). If possible, replacing them with automatic valves or a multiphase mixer would ensures a homogeneous dispersion of the phases. Also operating it remotely would allow for better control in case of water carryover to the atmospheric distillation column downstream.

Reduction of demulsifier consumption: By adjusting the pH-concentration sweep (Fig. **2**) and physically relocating the chemical injection to the inlet line of the cold preheating train (ensuring extended contact time, see Fig. **A5** in Appendix), field dosing was reduced to an optimal range of 6 to 10 ppm under full feed load (247 MBPSD, 100 °F, 448 psig).

Regularization of wash water flow: The installation of an automated globe valve with a control loop was planned to manage the flow coming from the vacuum section surge drum, ensuring a continuous delivery of 100 gpm to the second stage. With the sizing, the flow coefficients (Cv) and openings were estimated: minimum of 8.4 (31.9%), normal of 17.8 (56.4%), and maximum of 19.9 (62.0%).

Test plan to remove sludge deposits from the bottom of desalters: Waste management is important for the proper operation of process units and for meeting environmental regulations. In the desanders, the sludge that forms at the bottom of the containers is a suspension of solids in water that causes deposits, takes up space, and disrupts the process. Due to sampling limitations (available only in first-stage desanders), a hydraulic test is proposed, varying the wash time per tap in each line (7, 9, and 11 minutes) and the wash water pressure (235 to 240 psig).

4.5. Industrial Implications

The optimization of the operational parameters evaluated in this study has a direct impact not only on the integrity, stability, and sustainability of the desalting system, but also on downstream equipment like the atmospheric distillation unit, which suffers the consequences of poor desalting. A 50 PTB reduction in salt content means a 12% improvement in desalting efficiency (see Table **4**). This action reduces the formation of hydrochloric acid from the hydrolysis of chloride and magnesium salts, as well as its corrosive effect on the top of the fractionation column, which can lead to premature metallurgical failures and even the collapse of the unit.

The reconfiguration of the control loops in the Distributed Control System (DCS) allows responding to stochastic disturbances in the flow and changes in the crude feed. Automation stabilizes the operating level of the water-oil interface within the desalters, preventing carryover phenomena.

Strict control over the quality of wash water and the hydraulic purge cycles prevents sludge precipitation and compaction. As a result, the nominal hydraulic residence time of the equipment remains constant. It also reduces the failure rate due to mechanical abrasion in the effluent pumping systems.

Conditioning the acidic wash water is crucial to prevent emulsion hydrocarbons from getting into the wastewater treatment unit. By making sure the effluent has oil and grease levels below the limit, the process meets environmental regulations and reduces the risk of exposure to hazardous volatile compounds in the facilities.

5. Conclusions

The evaluation of the desalting system shows a notable loss of process stability, attributed fundamentally driven by hydrodynamic and operational deviations. The resolution of the emulsion in the equipment's residence time requires a strict synergy of thermodynamic and transport properties to keep the fluid phases in a liquid state while meeting the requirements for heat and mass transfer combined with electrocoalescence. In combination, the interfacial physical chemistry of the demulsifier at the optimal concentration ensures efficient phase separation.

To overcome these operational challenges and restore hydrodynamic stability, a multivariable optimization strategy was implemented. It started with conditioning the wash water and adjusting the differential pressure to accommodate feed variations. Then, the conventional ball valve was replaced with a high-precision globe valve. This configuration prevents over-emulsification and guarantees appropriate mixing energy. Third, the process control philosophy was reconfigured within the Distributed Control System (DCS), replacing the single-feed loop with an automated low-selector and auto-manual station architecture to achieve strict hydraulic balance across both parallel desalting trains.

For future research work, the use of high-purity steam condensate could be considered as an alternative source of wash water, to take advantage of its low chloride content and the absence of volatile organic compounds. Additionally, systematic tank drainage protocols, automated monitoring of the interface level, and continuous tracking of critical thermodynamic parameters are recommended. These comprehensive actions establish an optimization framework capable of maximizing desalting efficiency and reducing maintenance in the crude upgrading circuit.

Conflict of Interest

The authors indicate that they have no conflict of interest.

Funding

The Universidad de Oriente funded this project.

Acknowledgments

The authors would like to thank the technical staff of the Universidad de Oriente, Servicios Enviroil C.A., and Petróleos de Venezuela S.A. for their support in the physicochemical analyses and experimental tests. To Alexis Cova-Bonillo, Ph.D., for his contribution to the drafting of the manuscript.

References

[1] Cottrell FG, Speed JB, inventors. Separating and collecting particles of one liquid suspended in another liquid. US patent US987115A. 1911 Mar 21.

[2] Waterman LC. Electric coalescers. Chem Eng Prog. 1965; 61(1): 51-7.

[3] Blumer D. Advanced electrostatic technologies for dehydration of heavy oils. In: Proceedings of SPE/PS-CIM/CHOA International Thermal Operations and Heavy Oil Symposium; 2005 Nov 1-3; Calgary, Alberta, Canada. Richardson (TX): Society of Petroleum Engineers; 2005. SPE-97786-MS. https://doi.org/10.2523/97786-MS

[4] Noïk C, Chen J, Dalmazzone C. Electrostatic demulsification on crude oil: a state-of-the-art review. In: International Oil & Gas Conference and Exhibition in China; 2006 Dec 5-7; Beijing, China. Richardson (TX): Society of Petroleum Engineers; 2006. SPE-103808-MS. https://doi.org/10.2118/103808-MS

[5] Aryafard E, Farsi M, Rahimpour M, Raeissi S. Modeling electrostatic separation for dehydration and desalting of crude oil in an industrial two-stage desalting plant. J Taiwan Inst Chem Eng. 2016; 58(Suppl C): 141-7. https://doi.org/10.1016/j.jtice.2015.06.028

[6] Mohammadi F, Mohammadi M, Nonahal B. A comprehensive electrical model for the electrostatic desalting process of crude oil. Pet Coal. 2019; 61(4): 738-48.

[7] Abdulredha MM, Hussain SA, Abdullah LC, Hong TL. Water-in-oil emulsion stability and demulsification via surface-active compounds: a review. J Pet Sci Eng. 2022; 209: 109848. https://doi.org/10.1016/j.petrol.2021.109848

[8] Salager JL. Bases fundamentales del papel de la química deshidratante: Influencia de la formulación fisicoquímica sobre la estabilidad de una emulsión. Rev Técnica INTEVEP. 1987; 7(1): 3-15. Reprinted in: Int J Chem Eng. 1990; 30(1): 103-16.

[9] Wu J, Xu Y, Dabros T, Hamza HA. Effect of demulsifier properties on destabilization of water-in-oil emulsion. Energy Fuels. 2003;17(6):1554-9. https://doi.org/10.1021/ef030113e

[10] Marfisi S. Estabilidad de emulsiones relacionada con el proceso de deshidratación de crudos [doctoral dissertation on the Internet]. Mérida: Universidad de Los Andes; 2005. Available from: https://www.ing.ula.ve/doctorado_ca/tesis2005.html

[11] Márquez R, Meza L, Alvarado JG, Bullón J, Langevin D, Forgiarini A, et al. Interfacial rheology measured with a spinning drop interfacial rheometer: particularities in more realistic surfactant-oil-water systems close to optimum formulation at HLDN = 0. J Surfactants Deterg. 2021; 24(4): 587-601. https://doi.org/10.1002/jsde.12502

[12] Salager JL, Forgiarini A, Bullón J, Delgado-Linares JG, Márquez R, Aubry J. Concepto de formulación y algunas de sus aplicaciones interfaciales en sistemas micro-heterogéneos surfactante/agua/aceite. In: Avances y Retos de la Ciencia e Ingeniería. Mérida: Universidad de Los Andes; 2019. Chapter 1, p. 1-14. Available from: https://www.researchgate.net/publication/335749912

[13] Aubry JM. Nouveaux paradigmes et nouveaux outils pour la formulation. In: 20èmes Journées de Formulation; 2021 Nov 29; Compiègne, France. HAL-03620012; 2021.

[14] Erzen B, Karatas M, Deniz S, Aydogmus E. Advances in synthesis, characterization, and industrial applications of phenol formaldehyde resins. Int J Adv Nat Sci Eng Res. 2024; 8: 26-34.

[15] Joseph J, Naiker V, Sreeram P, Mampulliyalil F, Varghese P, Dhawale P, et al. Phenolic resin: preparation, structure, properties, and applications. In: Raghavan P, Sreekala MS, Ravindran L, Menon A, Eds. Handbook of thermosetting foams, aerogels, and hydrogels. Elsevier; 2024. p. 383-420. https://doi.org/10.1016/B978-0-323-99452-1.00003-6

[16] Palacios P, Marfisi S, Moreno L, Obando Y. Síntesis de resinas fenol-formaldehido y su aplicación como dispersante y desemulsionante en emulsiones de petróleo pesado con asfaltenos floculados. Avances Quím. 2025; 20(2): 41-51. Available from: https://www.saber.ula.ve/avancesenquimica

[17] Salager JL, Márquez R, Delgado-Linares JG, Rondón M, Forgiarini A. Fundamental basis for action of a chemical demulsifier revisited after 30 years: (HLDN) as the primary criterion for water-in-crude oil emulsion breaking. Energy Fuels. 2022; 36(2): 711-30. https://doi.org/10.1021/acs.energyfuels.1c03349

[18] Saad MA, Kamil M, Abdurahman NH, Yunus R, Awad OI. An overview of recent advances in state-of-the-art techniques in the demulsification of crude oil emulsions. Processes. 2019; 7(7): 470. https://doi.org/10.3390/pr7070470

[19] Zhang F, Tan Z, Yu Z, Sima H, Wang Y, Zhang Y. Research status and analysis of stabilization mechanisms and demulsification methods of heavy oil emulsions. Energy Sci Eng. 2020; 8(12): 4158-77. https://doi.org/10.1002/ese3.814

[20] Raya SA, Mohd IA, Abbas AA, Abubakar AA. A critical review of development and demulsification mechanisms of crude oil emulsion in the petroleum industry. J Pet Explor Prod Technol. 2020; 10(4): 1711-28. https://doi.org/10.1007/s13202-020-00830-7

[21] Topilnytskyy P, Shyshchak M, Skorokhoda V, Torskyi V. Demulsification methods for heavy crude oil emulsions: a review. Chem Chem Technol. 2024; 18(2): 270-83. https://doi.org/10.23939/chcht18.02.270

[22] Li M, Yang D, Zhong H, Pan J, Cai L, Miao J, et al. Enhancing dewatering and desalting of crude oil: a comprehensive study on energy-efficient separation technology driven by electric-magnetic coupling field. Sep Purif Technol. 2025; 361: 131501. https://doi.org/10.1016/j.seppur.2024.131501

Chis T, Sterpu AE, Săpunaru OV. The effect of corrosion on crude oil distillation plants. ChemEngineering. 2022; 6(3): 41. https://doi.org/10.3390/chemengineering6030041

[23] Shattab S, Khudair W, Mohammed M, Kahthim M. Corrosion in crude oil distillation units (CDUs) and a study of reducing its rates by changing chemical injection sites. Pet Res Stud. 2023; 13(3): 143-61. https://doi.org/10.52716/jprs.v13i3.718

[24] ASTM D3230-13. Standard test method for salts in crude oil (electrometric method). West Conshohocken (PA): ASTM International; 2013.

[25] ASTM D4052-16. Standard test method for density, relative density, and API gravity of liquids by digital density meter. West Conshohocken (PA): ASTM International; 2016.

[26] ASTM D4007-22. Standard test method for water and sediment in crude oil by the centrifuge method (laboratory procedure). West Conshohocken (PA): ASTM International; 2022.

[27] Lipps WC, Baxter TE, Braun-Howland E. SM 4500-Cl: Chloride. In: American Public Health Association. Standard methods for the examination of water and wastewater. 24th ed. Washington (DC): APHA; 2023. https://doi.org/10.2105/SMWW.2882.079

[28] Lipps WC, Baxter TE, Braun-Howland E. SM 4500-H+: pH. In: American Public Health Association. Standard methods for the examination of water and wastewater. 24th ed. Washington (DC): APHA; 2023. https://doi.org/10.2105/SMWW.2882.082

[29] Lipps WC, Baxter TE, Braun-Howland E. SM 4500-S2-: Sulfide. In: American Public Health Association. Standard methods for the examination of water and wastewater. 24th ed. Washington (DC): APHA; 2023. https://doi.org/10.2105/SMWW.2882.096

[30] Baxter TE, Braun-Howland E, editors. SM 4500-NH3: Nitrogen (ammonia): a titrimetric method. In: American Public Health Association. Standard methods for the examination of water and wastewater. 24th ed. Washington (DC): APHA; 2023. https://doi.org/10.2105/SMWW.2882.096

[31] American Public Health Association, Baxter TE, Braun-Howland E, editors. SM 5520-C: Oil and grease. In: Standard methods for the examination of water and wastewater. 24th ed. Washington (DC): APHA; 2023. https://doi.org/10.2105/SMWW.2882.107

[32] Montgomery DC. Design and analysis of experiments. New Jersey: John Wiley & Sons; 2017.

[33] Antony J. Full factorial designs. In: Antony J, Ed. Design of experiments for engineers and scientists. 3rd ed. Oxford: Elsevier; 2023. p. 65-87. https://doi.org/10.1016/B978-0-443-15173-6.00009-3

[34] Salager JL. Formulation concepts for the emulsion maker. In: Nielloud F, Mestres G, Eds. Pharmaceutical emulsions and suspensions. New York: Marcel Dekker; 2000. p. 19-72. https://doi.org/10.1201/b14005-3

[35] Marfisi Valladares S, Lobo Poito MV, Guerrero AX, Carvajal Haddad C. Observación microscópica del proceso de formación y ruptura de emulsiones de crudos extrapesados de la Faja Petrolífera del Orinoco. Rev Latinoam Metal Mater. 2023; S10: 3-10. https://doi.org/10.5281/zenodo.17402395

[36] PDVSA. Procedimiento operacional N° J-E-OPR-010-10-IT-224: remoción de lodos en los desaladores. Caracas: PDVSA; 2009.

[37] Vafajoo L, Ganjian K, Fattahi M. Influence of key parameters on crude oil desalting: an experimental and theoretical study. J Pet Sci Eng. 2012; 90: 107-11. https://doi.org/10.1016/j.petrol.2012.04.022

[38] Abdalla B, Gasmseed G, Elnour M, Ahmed A. Optimum electrostatic desalting efficiency of Alfulla crude oil. Eng Comput Sci. 2015; 16(1): 56-62.

[39] Sellami MH, Naam R, Temmar M. Optimization of operating parameters of oil desalting in Southern treatment unit (HMD/Algeria). J Pet Environ Biotechnol. 2016;7(2):1000271. https://doi.org/10.4172/2157-7463.1000271

[40] Tang L, Wang T, Xu Y, He X, Yan A, Zhang Z, et al. Research and application progress of crude oil demulsification technology. Processes. 2024; 12: 2292. https://doi.org/10.3390/pr12102292

[41] Becher P. Emulsions: theory and practice. New York: Reinhold Publishing Corporation; 1966. p. 440.

[42] Eow JM, Ghadiri M. Electrostatic enhancement of coalescence of water droplets in oil: a review of current understanding. Chem Eng J. 2001; 84: 173-92. https://doi.org/10.1016/S1385-8947(00)00386-7

[43] Pedersen A. Forces acting on water droplets in electrically energized oil emulsions: observation and modelling of droplet movement leading to electrocoalescence [doctoral dissertation]. Trondheim: Norwegian University of Science and Technology; 2008. Available from: https://www.osti.gov/etdeweb/biblio/974382

[44] Marfisi S, Álvarez G, Paruta E, Moreno P, Antón R, Salager J. Deshidratador electrostático de laboratorio para probar formulaciones desemulsionantes. Rev Cienc Ing. 2009; 30(3): 229-36. Available from: http://www.redalyc.org/articulo.oa?id=507550786007

[45] Al-Otaibi M, Elkamel A, Al-Sahhaf T, Ahmed AS. Experimental investigation of crude oil desalting and dehydration. Chem Eng Commun. 2003; 190(1): 65-82. https://doi.org/10.1080/00986440302094

[46] Centeno-Bordones G, Labrador H, Lara-Moreno G. Sour waters in heavy crude oil processing: physicochemical characterization and prognosis of its environmental impact. Novasinergia. 2021; 4(1): 115-35. https://doi.org/10.37135/ns.01.07.07

[47] Nasehi S, Javad Sarraf M, Ilkhani A, Mohammadmirzaie M, Hasan Fazaelipoor M. Statistical evaluation and optimization of crude oil desalting unit: a case study of Bandar Abbas oil refinery. J Biochem Technol. 2019; Especial 2: 59-68.

[48] Casas J, González M, Marfisi N. Interpretación de facies genéticas en pozos verticales/inclinados/horizontales y su integración en el modelo geológico. Formación Oficina, campo Sincor, Bloque Junín, Faja Petrolífera del Orinoco, Venezuela. In: IX Congreso Geológico Venezolano; 2007; Caracas, Venezuela. Available from: https://www.researchgate.net/publication/249657392_Interpretacion_de_facies_geneticas_en_pozos_verticalesinclinadoshorizontales_y_su_integracion_en_el_modelo_geologico_Formacion_Oficina_Campo_Sincor_Bloque_Junin_Faja_Petrolifera_del_Orinoco_Venezuela

[49] Carnegie A, Mathews S, O'Keefe M, Raghuraman B, Wei W, Gang C. Finding value in formation water. Oilfield Rev. 2011; 23(1): 24-35. Available from: https://www.slb.com/-/media/files/oilfield-review/finding-value

Appendix

Table A1: Characterization of the diluted crude oil samples and wash water

Parameter	Method	Value
Salt concentration in feed crude (PTB)	ASTM D3230	58.0 ± 0.01
Water and basic sediments in crude oil (% v/v)	ASTM D4007	1.9 ± 0.05
API gravity of feed crude (°API)	ASTM D4052	15.9 ± 0.01
Total acidity of feed crude (mg KOH/g)	ASTM D664	3.4 ± 0.01
Chloride concentration in sour wash water (mg/L)	SM 4500 Cl	54.6 ± 0.01
pH of sour wash water (electrometric method)	SM 4500-H+	9.1 ± 0.01
Oils and fats in sour wash water (mg/L)	SM 500-C	58,1± 0.01
Hydrogen sulfide content in sour water (mg/L)	SM 4500-S^{2-}	64,6 ± 0.01
Ammoniacal nitrogen content in sour water (mg/L)	SM 4500-NH_3	477 ± 0.01

Table A2: Validation of the computational tool with the design and operational values

Parameter	Unit	Experimental	Calculated	%Error
Salt content in the crude 2nd stage (design)	PTB	2.00	2.00	0.00
Salt content in the crude 1st stage (operational)	PTB	13.00	13.12	0.92
Salt content in the crude 2nd stage (operational)	PTB	9.50	10.00	5.26

Table A3: Pressure and temperature conditions in the crude oil desalters

	First stage of crude desalting		Second stage of crude desalting	
Variable	D1A	D1B	D2A	D2B
Design pressure (psig)	165.0	140.0	165.0	140.0
Operating pressure (psig)	127.0	110.0	127.0	108.0
Operating temperature (°F)	281.4	280.9	279.6	279.2
Design temperature (°F)	307.0	300.0	307.0	300.0
Pressure at the train inlet (psig)	146.1	-	146.1	-
Pressure drop in mixing valves (psi)	15.7	15.7	14.8	13.6

Figure A1: One-dimensional scans of pH and demulsifier concentration (180 °F, 14.7 psi).

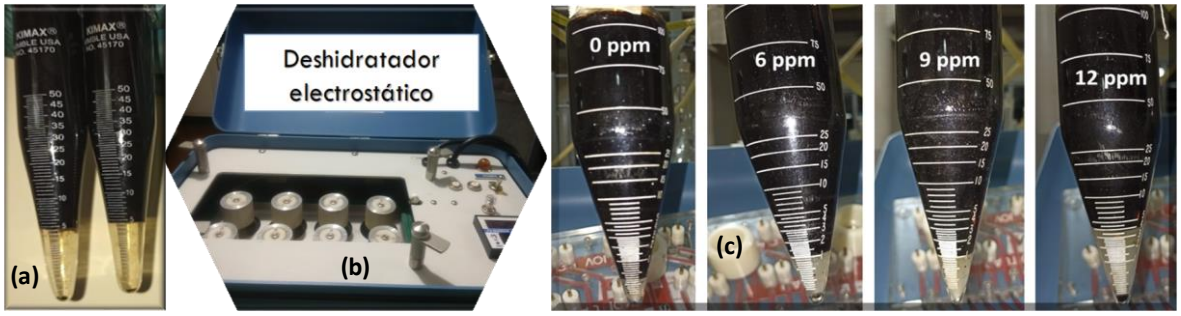

Figure A2: Efficiency test with an electrostatic dehydrator under simulated field conditions (3 kV, 180 °F, 14.7 psi) and pH adjustment of the wash water before forming the W/O emulsion with heavy crude oil. a) Measurement of initial basic sediment and water content (%BSW), b) Execution of the test in the treater equipment; c) Water separated in the graduated cylinders at the end of the assay.

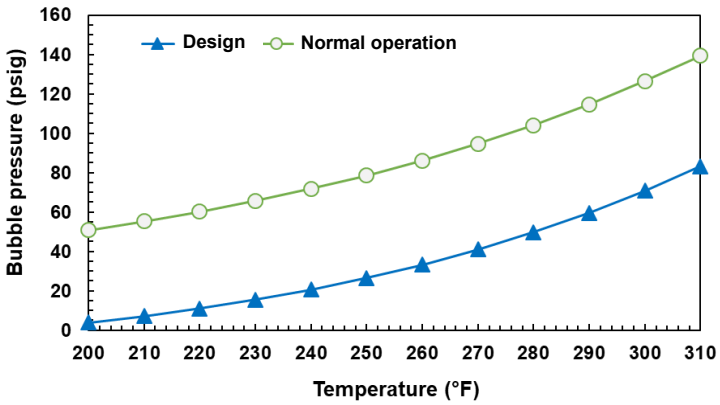

Figure A3: Variation of the bubble point pressure with temperature in the desalters, considering the crude oil composition at design and normal operating conditions.

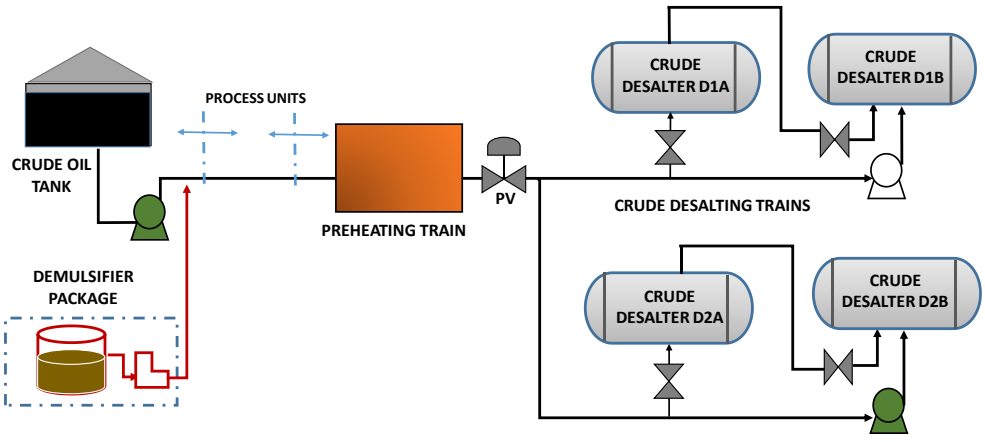

Figure A4: Simplified diagram with the preliminary location of the demulsifier injection point in the tank farm of the crude oil upgrader.